Original Investigation

Role of the Medial Prefrontal Cortex in Impaired Decision Making in Juvenile Attention-Deficit/Hyperactivity Disorder

Tobias U. Hauser, PhD; Reto Iannaccone, MS; Juliane Ball, PhD; Christoph Mathys, PhD; Daniel Brandeis, PhD; Susanne Walitza, MD; Silvia Brem, PhD

IMPORTANCE Attention-deficit/hyperactivity disorder (ADHD) has been associated with deficient decision making and learning. Models of ADHD have suggested that these deficits could be caused by impaired reward prediction errors (RPEs). Reward prediction errors are signals that indicate violations of expectations and are known to be encoded by the dopaminergic system. However, the precise learning and decision-making deficits and their neurobiological correlates in ADHD are not well known.

OBJECTIVE To determine the impaired decision-making and learning mechanisms in juvenile ADHD using advanced computational models, as well as the related neural RPE processes using multimodal neuroimaging.

DESIGN, SETTING, AND PARTICIPANTS Twenty adolescents with ADHD and 20 healthy adolescents serving as controls (aged 12-16 years) were examined using a probabilistic reversal learning task while simultaneous functional magnetic resonance imaging and electroencephalogram were recorded.

MAIN OUTCOMES AND MEASURES Learning and decision making were investigated by contrasting a hierarchical Bayesian model with an advanced reinforcement learning model and by comparing the model parameters. The neural correlates of RPEs were studied in functional magnetic resonance imaging and electroencephalogram.

RESULTS Adolescents with ADHD showed more simplistic learning as reflected by the reinforcement learning model (exceedance probability, P_x = .92) and had increased exploratory behavior compared with healthy controls (mean [SD] decision steepness parameter β: ADHD, 4.83 [2.97]; controls, 6.04 [2.53]; P = .02). The functional magnetic resonance imaging analysis revealed impaired RPE processing in the medial prefrontal cortex during cue as well as during outcome presentation (P < .05, family-wise error correction). The outcome-related impairment in the medial prefrontal cortex could be attributed to deficient processing at 200 to 400 milliseconds after feedback presentation as reflected by reduced feedback-related negativity (ADHD, 0.61 [3.90] μV; controls, −1.68 [2.52] μV; P = .04).

CONCLUSIONS AND RELEVANCE The combination of computational modeling of behavior and multimodal neuroimaging revealed that impaired decision making and learning mechanisms in adolescents with ADHD are driven by impaired RPE processing in the medial prefrontal cortex. This novel, combined approach furthers the understanding of the pathomechanisms in ADHD and may advance treatment strategies.

+ **Supplemental content** at jamapsychiatry.com

Author Affiliations: Author affiliations are listed at the end of this article.

Corresponding Author: Tobias U. Hauser, PhD, University Clinics for Child and Adolescent Psychiatry, University of Zurich, Neumünsterallee 9, 8032 Zürich, Switzerland (tobias.hauser @kjpd.uzh.ch).

A ttention-deficit/hyperactivity disorder (ADHD) has been associated with deficits in decision making and learning.[1] These skills are guided by the dopaminergic system,[2] which is impaired in ADHD.[3-5] However, little is known about the cortical mechanisms and processes that cause these deficits.[1] Several influential ADHD models[6-8] suggest that these decision-making and learning impairments are caused by impaired processing of what are termed *reward prediction errors* (RPEs).

Reward prediction errors have been discovered to reflect neural signals that drive learning and decision making.[2,9,10] Reward prediction errors signal violations of expectations and can be estimated by using computational reinforcement learning models.[11] It is now widely accepted that RPE signals are encoded by the phasic firing rate of dopaminergic neurons in the mesencephalon.[12] Reward prediction errors occur at 2 points during a decision-making trial: at cue and at outcome presentation. At cue presentation, RPEs (RPE_{cue}) reflect the expected value of a selected stimulus. At outcome, the RPE ($RPE_{outcome}$) is the difference between the reward received and the expected value of the selected stimulus.[13] These RPE signals are projected from the dopaminergic midbrain to several prefrontal and striatal areas that are also crucially involved in decision making, such as the ventral striatum and the medial prefrontal cortex (mPFC).[8,14,15] Neuroimaging studies[16-19] have consistently identified these regions as being impaired in ADHD. Additionally, studies on feedback-related negativity (FRN),[20-22] an electroencephalogram (EEG) component reflecting RPE processing in the mPFC, have suggested that RPE processing may be impaired as early as 200 to 400 milliseconds after outcome presentation in ADHD.[23-26]

Although several lines of evidence suggest RPE impairments in ADHD, no study has investigated the neural substrates of RPE processing by means of computational modeling of learning and decision making in juvenile ADHD.

Additionally, it remains unknown how these RPE impairments may relate to deficient learning mechanisms. Computational simulations of ADHD behavior[27] have suggested that individuals with ADHD make more exploratory decisions or may have a reduced learning rate, but this has not been examined in patients.

In this study, we applied the novel methods of computational psychiatry.[28] Computational psychiatry uses biologically plausible models, such as the aforementioned RPE-based reinforcement learning models,[11] to understand the mechanisms that underlie disturbed learning and decision making and overcome the limitations of purely descriptive measures, such as error rates. We examined the neural correlates of RPE processing. To overcome the poor temporal resolution of functional magnetic resonance imaging (fMRI) and the weak spatial resolution of EEG,[29] we used a simultaneous EEG-fMRI approach that exploits the advantages of both modalities without relying on spatial or other constraints of separate analyses.[30-32]

Methods

Participants

The study was approved by the ethics committee of the Canton of Zurich, Switzerland, and all participants and their parents gave written informed consent. The participants each received a voucher for local stores for their participation.

Forty adolescents aged 12 to 16 years participated in this study (**Table 1**). Twenty individuals with ADHD were recruited from our outpatient clinics. Twenty healthy adolescents were recruited from local schools to serve as controls. All participants underwent a semistructured clinical interview (Schedule for Affective Disorders and Schizophrenia for School-Age Children–Present and Lifetime Version, German

Table 1. Characteristics of the Participants

Characteristic[a]	Control Group	ADHD Group	Significance
Age, mean (SD), y	14.80 (1.46)	14.60 (1.67)	$t_{38} = .41; P = .69$
Sex (male/female), No.	10/10	13/7	$\chi_1^2 = .92; P = .34$
Handedness (left/right), No.[b]	1/19	4/16	$\chi_1^2 = 2.06; P = .15$
IQ estimate, mean (SD)[c]	113 (11)	108 (16)	$t_{38} = 1.22; P = .23$
WISC score (standardized), mean (SD)			
Block design	12.4 (2.4)	12.0 (3.6)	$t_{38} = 0.37; P = .72$
Similarities	11.9 (1.4)	11.3 (1.7)	$t_{38} = 1.31; P = .20$
Digit span	10.5 (2.4)	9.5 (3.0)	$t_{38} = 1.13; P = .27$
ADHD index, mean (SD)[d]	49.5 (6.1)	67.4 (7.5)[e]	$t_{38} = -8.22; P < .001$
Medication	NA	Methylphenidate (n = 14), isotretinoin (n = 1), melatonin (n = 1)	NA
Past or current comorbidities[f]	Transient tic (n = 3), affective disorders (n = 1), phobias and other anxiety disorders (n = 3), enuresis (n = 1)	Transient tic (n = 4), affective disorders (n = 6), phobias and other anxiety disorders (n = 3), enuresis (n = 1), learning and developmental disorders (n = 4), conduct disorder (n = 3)	NA

Abbreviations: ADHD, attention-deficit/hyperactivity disorder; NA, not applicable; WISC, Wechsler Intelligence Scale for Children.

[a] Both groups were matched for age, sex, handedness, and intelligence, but differed significantly in the ADHD index of the Conners 3 questionnaire.

[b] According to Oldfield.[33]

[c] IQ was estimated based on the WISC subtests[34]; the IQ estimate was calculated using model 56 by Waldmann.[35]

[d] Derived from a research version of the Conners-3 scale; T values reported.[36]

[e] Missing data on 1 patient.

[f] As assessed by the Schedule for Affective Disorders and Schizophrenia for School-Age Children–Present and Lifetime Version.

Figure 1. Probabilistic Reversal Learning Task and Winning Computational Model
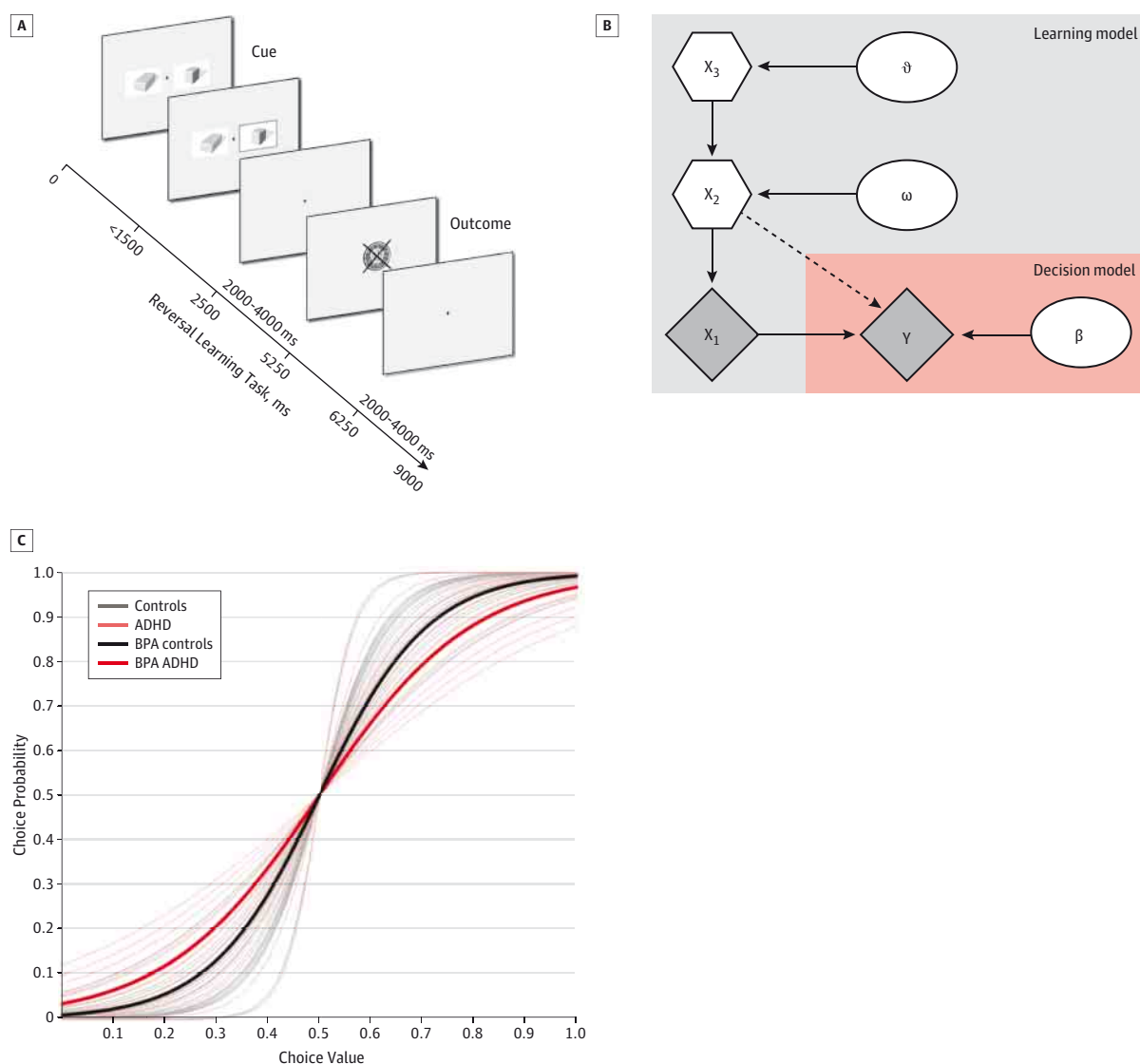
A, The participants played a probabilistic reversal learning task while simultaneous electroencephalogram and functional magnetic resonance imaging were recorded. In each trial, the participants had to select 1 of 2 stimuli: one had a reward probability of 0.8 and the other had a reward probability of 0.2. The participants had to learn the reward probabilities and detect reversals on a trial-and-error basis. B, The hierarchical Gaussian filter model performed best for the healthy controls, but not for the participants with attention-deficit/hyperactivity disorder (ADHD). Markovian states are denoted by x_1 to x_3, ϑ, ω, and β describe the free parameters. C, Group difference of the decision steepness parameter β indicates increased exploratory behavior in participants with ADHD compared with the controls. BPA indicates Bayesian parameter average.

version).[37,38] All participants with ADHD fulfilled the diagnosis of a combined inattention and hyperactivity-impulsivity subtype (*DSM-IV* code 314.01), corresponding to the 314.01 combined presentation according to *DSM-5*. Exclusion criteria were severe psychiatric disorders, such as schizophrenia, major depression, obsessive-compulsive disorder, pervasive developmental disorders, Tourette syndrome, substance abuse, primary mood or anxiety disorder (assessed using the Schedule for Affective Disorders and Schizophrenia for School-Age Children–Present and Lifetime Version), and autism spectrum disorders (assessed using the Social Communication Questionnaire[39]). At the time of our study, only 1 participant

with ADHD met the diagnostic criteria for comorbid conduct disorder, and none had oppositional defiant disorder. The controls were matched for age, sex, handedness, and IQ. Medicated patients with ADHD had to suspend their medication for at least 48 hours before testing. Because of excessive movement during scanning (>1 voxel maximal scan-to-scan movement), we had to exclude 1 participant with ADHD.

Procedures
Task
The participants played a probabilistic reversal learning task (**Figure 1**A and eMethods in the Supplement).[15,40] The partici-

pants had to learn the stimulus with a higher outcome probability on a trial-and-error basis to gain as much money as possible. The reward probabilities changed occasionally, and the participants had to adjust accordingly.

Computational Models

To infer learning, we compared 2 learning models and 2 decision models. As a standard learning model, we used an advanced Rescorla-Wagner model with an anticorrelated valuation system.[15] This model has been shown[15,40] to be highly successful at inferring learning in probabilistic reversal learning tasks. We compared this model with a flexible Bayesian learning model, the hierarchical Gaussian filter model (HGF).[41]

In essence, the 2 learning models differ in their flexibility of learning. The advanced Rescorla-Wagner model has a fixed learning rate across the whole experiment, which means that the values of the stimuli are constantly updated, irrespective of any environmental or other change. The HGF, in contrast, has a flexible learning rate that adapts to changes in the volatility of the environment and according to beliefs about the value of the objects. This assumes a more precise and fine-grained learning process and has been shown[42,43] to be superior to reinforcement learning models. These findings also imply that healthy individuals learn in a more sophisticated manner than is assumed by the more simplistic Rescorla-Wagner learning model.

To ensure that all participants understood the task and performed above chance level, we additionally compared the best-fitting model for each person with a model that assumes performance at chance level. One participant with ADHD had to be excluded from further analysis because the chance model outperformed the other models. A more detailed description of the models and their update equations is provided in eMethods in the Supplement.

To determine the model that fitted behavior optimally, we performed Bayesian model selection for groups[44] across all participants and for each group independently. To further investigate learning and decision-making impairments, we compared the parameter estimates of the model that performed best across all subjects using Mann-Whitney tests.

Simultaneous EEG-fMRI

Simultaneous EEG-fMRI was recorded (Achieva 3.0T scanner; Philips) using an MR-compatible EEG system (BrainAmp MR Plus; BrainProducts). Preprocessing and analysis of the fMRI were performed using SPM8 (http://www.fil.ion.ucl.ac.uk/spm/). Data obtained with EEG were preprocessed and analyzed using BrainVision Analyzer, version 2.0.2, and EEGLAB toolbox.[45] To study the neural differences in RPE processing between the groups as captured by fMRI, we entered the model-derived RPE values for every trial into the first-level analysis as 2 separate parametric modulators at the times of cue and outcome presentations. The first regressor corresponded to the RPE_{cue} and was therefore entered during cue presentation, whereas the second regressor modulated $RPE_{outcome}$ and was thus entered during outcome presentation. To study the group differences of RPE_{cue} and $RPE_{outcome}$, we used independent-sample t tests and a mul-

tiple comparison correction threshold of $P < .05$ cluster-extent family-wise error corrected (voxel-height threshold, $P < .001$). As ADHD diagnoses imply, individuals with ADHD also display increased motor activity. Because the scan-to-scan motion differed marginally between our groups (ADHD mean [SD]: 0.10 mm [0.03]; range, 0.05-0.15 mm; and controls: 0.08 mm [0.03]; range, 0.05-0.20 mm; t_{36}, −2.0; $P = .052$), and because we wanted to ensure that our findings were not biased by movement artifacts, we also decided to analyze reduced groups excluding the 6 adolescents with the highest mean scan-to-scan movements (5 ADHD and 1 control). The reduced groups no longer differed significantly in motion ($P > .10$), and we subsequently discuss only the findings that were consistent across both analyses.

In the EEG, the FRN was analyzed as the difference between the most negative peak between 200 and 425 milliseconds after feedback and the preceding positive peak between 150 and 300 milliseconds (eFigure 1 in the Supplement).[46] These peaks were determined for each condition (reward and punishment) and participant separately. The FRN was then computed as the difference between punishments and rewards.

To localize the FRN, we used an EEG-informed fMRI approach[30,32,40] and entered the single-trial amplitudes as parametric modulators during feedback presentation into the first-level fMRI analysis. A detailed description of the preprocessing and data analysis is provided in the eMethods in the Supplement.

Results

Behavior

Mean reaction times, reaction time variability, and the number of misses did not differ between the groups (eTable 1 in the Supplement). However, participants with ADHD earned marginally less than controls (ADHD, 10.30 [11.70] CHF; controls, 15.60 [5.65] CHF; $t_{38} = 1.82$; $P = .08$).

Behavioral Model Comparison

Using Bayesian model selection for groups,[44] we found that the HGF performed best across all subjects ($P_x = .70$; P_x is the exceedance probability, ie, the probability that this particular model performs better than any other model included in the comparison) (eTable 2 in the Supplement and Figure 1B). The HGF also performed best for the controls ($P_x = .98$). For ADHD, however, the anticorrelated Rescorla-Wagner model clearly outperformed the HGF ($P_x = .92$).

Model Parameter Comparison

The model parameter comparison of the best-performing model across all participants (HGF) revealed that those with ADHD showed a significantly less steep decision function (β: ADHD, 4.83 [2.97]; controls, 6.04 [2.53]; $U = 109$; $z = −2.276$; $P = .02$) (Figure 1C). We found no significant differences between the groups for the subject-specific volatility estimate (ω: ADHD, −1.70 [1.60]; controls, −1.26 [0.40]; $U = 187$; $z = −0.08$; $P = .95$) or the meta-volatility parameter (ϑ: ADHD, 0.0025 [0.0001]; controls, 0.0025 [0.0001]; $U = 166$; $z = −0.674$; $P = .51$).

Table 2. Group Differences Between Patients With ADHD and Healthy Adolescents for RPE$_{cue}$ and RPE$_{outcome}$ [a]

Contrast	Region	Hemisphere	Cluster Size (Voxels)	x	y	z	z Score
Controls > ADHD							
RPE$_{cue}$	NS						
RPE$_{outcome}$	ACC	Right	106	24	33	15	4.48
	mPFC	**Bilateral**	**406**	**−8**	**54**	**18**	**4.35**
		Left	200	−8	48	42	4.16
	MTG	Right	1094	51	−39	2	4.29
	STG	Left	170	−65	−54	18	4.27
			234	−56	−24	−5	4.26
			123	−36	−6	−11	3.94
	SMG	Right	192	71	−30	30	4.24
		Left	204	−57	−28	21	3.85
	MFG	Right	134	26	15	21	3.95
	Precentral	Right	142	57	−7	45	3.76
	Lingual	Right	151	20	−55	−9	3.75
ADHD > Controls							
RPE$_{cue}$	**mPFC**	**Right**	**128**	**8**	**66**	**15**	**4.72**
RPE$_{outcome}$	NS						

Abbreviations: ACC, anterior cingulate cortex; ADHD, attention-deficit/hyperactivity disorder; MFG, middle frontal gyrus; mPFC, medial prefrontal cortex; MTG, middle temporal gyrus; NS, no significance; RPE, reward prediction error; SMG, supramarginal gyrus; STG, superior temporal gyrus.

[a] Boldface type regions indicate that the difference remained significant in the comparison of the reduced groups. Significance threshold was set to $P < .05$ cluster-extent family-wise error correction. Coordinates are reported in Montreal Neurological Institute space.

Neural Group Differences in RPE Processing

During cue presentation (RPE$_{cue}$), participants with ADHD were found to process RPEs significantly differently in the mPFC (**Table** 2 and **Figure** 2A), both in the analysis containing all subjects and in the reduced groups.

During outcome presentation (RPE$_{outcome}$), RPE processing consistently elicited differential activations in the mPFC, both in the analysis containing all participants and in the reduced groups (Table 2 and Figure 2B). Additional group differences in the complete sample (Table 2) did not remain significant in the reduced groups.

Temporal Aspects of RPE Processing: FRN

The amplitudes for rewards and punishments were found to be largest at electrode Fz (eResults in the Supplement). The FRN at this electrode was significantly larger in the control group than that for the participants with ADHD (controls, −1.68 [2.52] μV; ADHD, 0.61 [3.90] μV; $t_{36} = −2.17$; $P = .04$) (**Figure** 3A). Further analyses revealed that the controls showed a significant FRN ($t_{19} = −2.98$; $P = .008$), whereas the participants with ADHD did not ($t_{17} = 0.66$; $P = .52$).

Localization of the FRN

To determine the generator of the FRN, we entered the single-trial amplitudes of the FRN as a parametric modulator in the fMRI design matrix. For the healthy controls, we localized the FRN to a cluster in the mPFC (Montreal Neurological Institute: x = −11, y = 56, z = 24; k̂ = 582; $z = 3.61$) (Figure 3B). For the adolescents with ADHD, we did not find any significant activation. Strikingly, the source of the FRN in the controls overlapped with the region that also shows a significant difference between the groups in the RPE$_{outcome}$ contrast.

Discussion

In this study, we provided insights into the dysfunctional decision-making and learning mechanisms in adolescent ADHD using advanced learning models in combination with simultaneously recorded EEG and fMRI data.

By using different computational models of learning, we found that the behavior of healthy controls was better explained by the more-flexible Bayesian HGF model, whereas the simpler Rescorla-Wagner model was better suited for the participants with ADHD. The 2 models differ mainly in their flexibility. The Rescorla-Wagner model has a fixed learning rate, which entails that RPEs always have the same effect on learning, and the HGF has a more flexible learning rate that builds on environmental volatility and the participants' current beliefs about the value of the objects. This diverging model selection result does not imply that the groups use strongly diverging learning mechanisms or diverging cognitive strategies. Rather, it suggests that adolescents with ADHD do not profit from the increased flexibility of the HGF and that they are not sensitive to subtle changes in reward contingencies, such as changes in environmental volatility or their current beliefs.

Comparison of the model parameters revealed that adolescents with ADHD have a less steep decision parameter β. This means that these participants differ in the exploration-exploitation dimension.[47,48] Participants with ADHD seem to exploit the best option less frequently according to their inferred beliefs, but to behave in a more exploratory way and examine the alternative option more often. This finding fits nicely with previous computational simulations,[27] which suggested that this decision steepness can cause ADHD-like behavior. In

Figure 2. Main Effects and Group Differences in Reward Prediction Error (RPE) Processing During Cue and Outcome Presentation
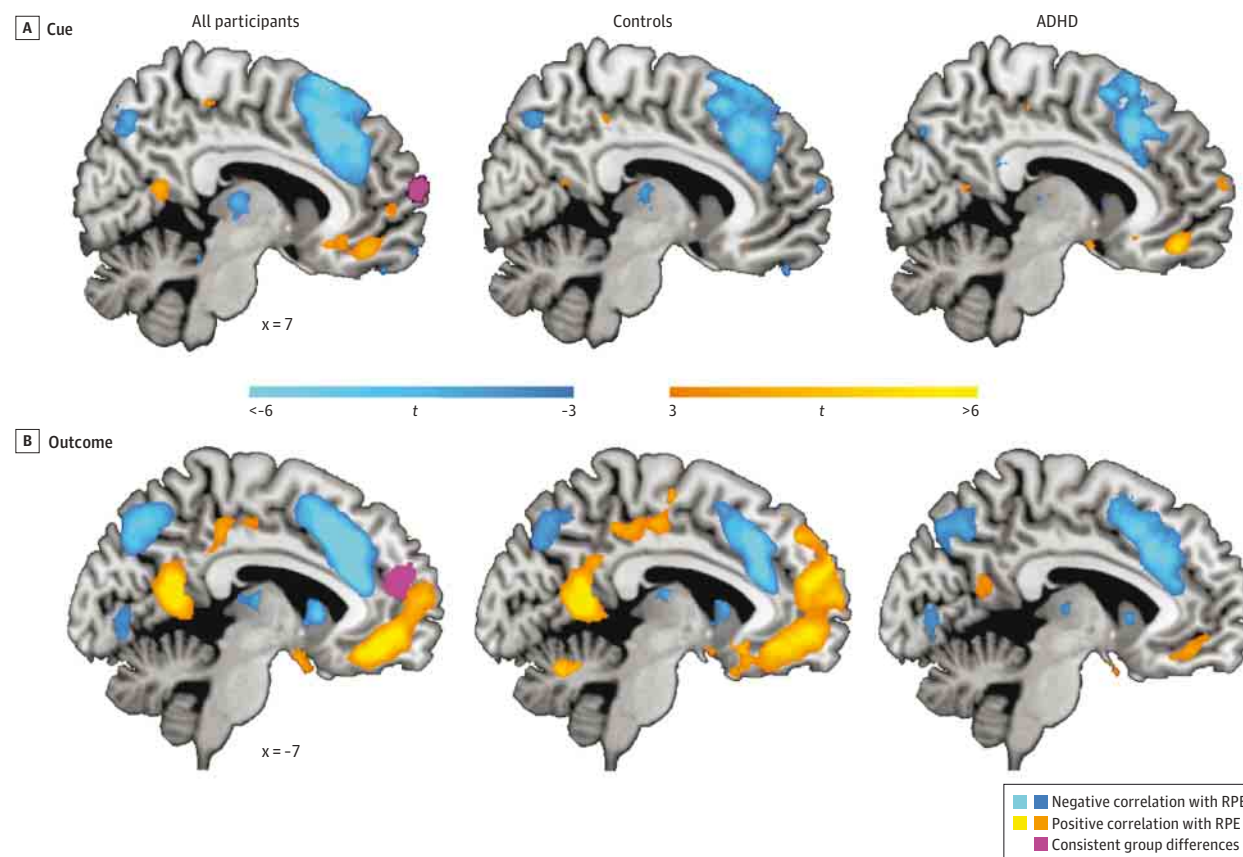
Groups showed a different response during cue (A) and outcome (B) in the medial prefrontal cortex. ADHD indicates attention-deficit/hyperactivity disorder.

decision making during uncertainty, exploratory behavior is crucial to success because it facilitates the detection of changes in reward contingencies.[47,48] However, the fact that the healthy controls earned marginally more implies that the exploratory behavior of the participants with ADHD was too high for optimal task performance and that they were not able to adequately adjust their exploratory behavior.

Our analysis further revealed that ADHD cannot be characterized by an altered learning rate per se, because the higher-order volatility parameters (ϑ, ω) do not differ. This is in line with a previous study that did not find any learning rate impairments in ADHD.[49] Our finding also indicates that the differences in the model selection are not primarily caused by the volatility estimate, but rather by the current belief about the value. This finding also confirms that the participants with ADHD learned the reward contingencies properly and that the increased exploratory behavior found in the present study does not simply reflect randomness in behavior.

To understand the neural mechanisms that are responsible for the changes in the decision-making and learning processes, we examined RPE processing during cue and outcome presentations between the groups. Critically, we found activation differences during both phases in adjoining regions in the mPFC. This finding fits neatly with our behavioral finding of an

altered decision steepness in ADHD, because we found the mPFC to be part of a network that is correlated with the decision-steepness parameter β in our participants (eResults, eTable 3, and eFigure 2C-D in the Supplement). Moreover, the mPFC is well known for processing prediction errors[50,51] and guiding value comparison and response selection,[52-54] and has been suggested to be a locus of malfunctioning decision making in ADHD.[8] Although the findings in previous studies[55,56] on reversal learning tasks in ADHD were not consistent regarding mPFC impairment, overall, this region has frequently been associated with neural alterations in ADHD during rest[57] and cognitive tasks.[16] Our findings indicate that deficient RPE processing in the mPFC may cause the suboptimal choice selection that is reflected by their more exploratory behavior.

The regions in the mPFC that we found to be impaired in ADHD are adjacent to the core regions known to process RPEs (Figure 2A and B). This suggests that individuals with ADHD may not process RPEs differently in the RPE core regions. Rather, it seems as if RPEs are processed in a less-extended area. This is also in line with our behavioral findings that learning in ADHD is not completely impaired; rather, there are more subtle differences, as reflected by the lowered decision steepness.

To better understand the temporal characteristics of RPE processing, we analyzed the FRN using an EEG-fMRI integra-

tion approach. We found that participants with ADHD did not have a significant FRN in contrast to the healthy controls, who showed a clear FRN. We successfully localized the FRN to the mPFC in healthy controls. Remarkably, the source of the FRN overlapped with the RPE$_{outcome}$ impairment in the participants with ADHD. This may explain why we did not find a significant FRN and were not able to localize the component in the ADHD group. It also suggests that the impairment in the mPFC in ADHD reflects an early cognitive deficiency that occurs less than 400 milliseconds after feedback. Research[23-25] so far has investigated the FRN in ADHD with mixed results. Our study not only adds additional evidence for FRN attenuation but also clarifies its role and the neural origin.

Given that previous studies[16,17,19] on ADHD have often focused on the ventral striatum, a region also known to process RPEs,[58-60] we performed a supplemental analysis of a cluster in the subgenual anterior cingulate cortex and ventral striatum, which was found to be active in our RPE analysis (eResults in the Supplement). We found no RPE-related difference between the groups during cue presentation, but significantly deficient RPE processing occurred in the ADHD group during the outcome (eFigure 3 in the Supplement). A connectivity analysis revealed that the connectivity between this region of interest and the mPFC$_{outcome}$ cluster is significantly lowered in ADHD. This finding indicates that both regions belong to a single frontostriatal loop, which has impaired connectivity in ADHD.
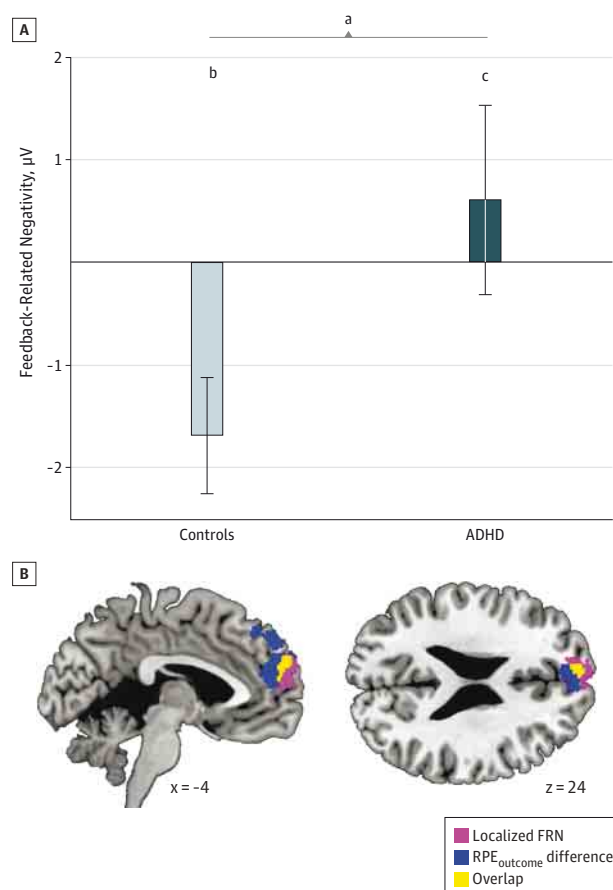
Attention-deficit/hyperactivity disorder has been discussed in the context of developmental delays.[61-66] Although our study cannot answer whether our findings reflect a developmental delay or an age-independent impairment, it is interesting that studies on healthy RPE development have found that the ventral striatum displays characteristic developmental trajectories[19,67,68] and that exploratory behavior decreases with age.[67]

A limitation of the present study is that most of our ADHD sample received methylphenidate. We interrupted the medication for the experiment and therefore ensured that our findings were not biased by acute medication effects. However, we cannot exclude the possibility that our findings were influenced by some long-term effects of the medication. We also decided to investigate individuals who had received medication because we think that untreated ADHD may represent a possibly less severely affected ADHD subgroup rather than a representative sample of the ADHD population.

Conclusions

Taken together, the results of the behavioral modeling, fMRI, and EEG data suggest that adolescents with ADHD have specific learning and decision-making deficits. Individuals with ADHD cannot be characterized by an impaired learning rate per se, in contrast to what has been suggested by theoretical models.[6,27] Rather, they show a less fine-grained decision process and explore more frequently. These impairments are most likely caused by impaired RPE processing in the mPFC, a well-known integrative hub in decision making and learning.

Figure 3. Temporal Aspects of Decision Making: the Feedback-Related Negativity (FRN)

A, Controls, but not participants with attention-deficit/hyperactivity disorder (ADHD), showed a significant FRN (punishment-reward) at electrode Fz. Mean values are presented; limit lines indicate SE. B, FRN was localized to the medial prefrontal cortex in the controls using an electroencephalogram-informed functional magnetic resonance imaging analysis. This cluster overlapped with the group difference in reward prediction error outcome (RPE$_{outcome}$), indicating that both measures depict the same impaired process (depicted at $P < .005$).

[a] $P = .04$.

[b] $P = .008$.

[c] $P = .52$.

By using a computational psychiatric approach[28] in combination with multimodal imaging, this study provides novel insights into impaired decision-making mechanisms and RPE deficits in adolescents with ADHD. Our findings further the understanding of potential pathomechanisms underlying impaired decision making and learning. Given that therapeutic interventions focus strongly on reinforcement modification, our findings could also inform interventional strategies for cognitive behavioral therapy (eg, working toward less-exploratory behavior). Moreover, our neural findings reinforce interventions in ADHD that focus on the mPFC, such as tomographic neurofeedback,[63] but may also encourage the use of extended neurofeedback methods, such as FRN-based training or real-time fMRI neurofeedback in the mPFC.

REFERENCES

1. Luman M, Tripp G, Scheres A. Identifying the neurobiology of altered reinforcement sensitivity in ADHD: a review and research agenda. *Neurosci Biobehav Rev*. 2010;34(5):744-754.

2. Schultz W. Getting formal with dopamine and reward. *Neuron*. 2002;36(2):241-263.

3. Volkow ND, Wang G-J, Kollins SH, et al. Evaluating dopamine reward pathway in ADHD: clinical implications. *JAMA*. 2009;302(10):1084-1091.

4. Sagvolden T. Behavioral validation of the spontaneously hypertensive rat (SHR) as an animal model of attention-deficit/hyperactivity disorder (AD/HD). *Neurosci Biobehav Rev*. 2000;24(1):31-39.

5. Swanson J, Baler RD, Volkow ND. Understanding the effects of stimulant medications on cognition in individuals with attention-deficit hyperactivity disorder: a decade of progress. *Neuropsychopharmacology*. 2011;36(1):207-226.

6. Tripp G, Wickens JR. Dopamine transfer deficit: a neurobiological theory of altered reinforcement mechanisms in ADHD. *J Child Psychol Psychiatry*. 2008;49(7):691-704.

7. Sagvolden T, Johansen EB, Aase H, Russell VA. A dynamic developmental theory of attention-deficit/hyperactivity disorder (ADHD) predominantly hyperactive/impulsive and combined subtypes. *Behav Brain Sci*. 2005;28(3):397-468.

8. Silvetti M, Wiersema JR, Sonuga-Barke E, Verguts T. Deficient reinforcement learning in medial frontal cortex as a model of dopamine-related motivational deficits in ADHD. *Neural Netw*. 2013;46:199-209.

9. Glimcher PW, Camerer CF, Fehr E, Poldrack RA. *Neuroeconomics: Decision Making and the Brain*. London, England: Elsevier; 2009.

10. Glimcher PW. Understanding dopamine and reinforcement learning: the dopamine reward prediction error hypothesis. *Proc Natl Acad Sci U S A*. 2011;108(suppl 3):15647-15654.

11. Sutton RS, Barto AG. *Reinforcement Learning: An Introduction*. Cambridge, MA: MIT Press; 1998.

12. Schultz W, Dayan P, Montague PR. A neural substrate of prediction and reward. *Science*. 1997;275(5306):1593-1599.

13. Niv Y, Edlund JA, Dayan P, O'Doherty JP. Neural prediction errors reveal a risk-sensitive reinforcement-learning process in the human brain. *J Neurosci*. 2012;32(2):551-562.

14. Bromberg-Martin ES, Matsumoto M, Hikosaka O. Dopamine in motivational control: rewarding, aversive, and alerting. *Neuron*. 2010;68(5):815-834.

15. Gläscher J, Hampton AN, O'Doherty JP. Determining a role for ventromedial prefrontal cortex in encoding action-based value signals during reward-related decision making. *Cereb Cortex*. 2009;19(2):483-495.

16. Bush G. Attention-deficit/hyperactivity disorder and attention networks. *Neuropsychopharmacology*. 2010;35(1):278-300.

17. Cubillo A, Halari R, Smith A, Taylor E, Rubia K. A review of fronto-striatal and fronto-cortical brain abnormalities in children and adults with attention deficit hyperactivity disorder (ADHD) and new evidence for dysfunction in adults with ADHD during motivation and attention. *Cortex*. 2012;48(2):194-215.

18. Cortese S, Kelly C, Chabernaud C, et al. Toward systems neuroscience of ADHD: a meta-analysis of 55 fMRI studies. *Am J Psychiatry*. 2012;169(10):1038-1055.

19. Plichta MM, Scheres A. Ventral-striatal responsiveness during reward anticipation in ADHD and its relation to trait impulsivity in the healthy population: a meta-analytic review of the fMRI literature. *Neurosci Biobehav Rev*. 2014;38:125-134.

20. Walsh MM, Anderson JR. Learning from experience: event-related potential correlates of reward processing, neural adaptation, and behavioral choice. *Neurosci Biobehav Rev*. 2012;36(8):1870-1884.

21. Holroyd CB, Coles MGH. The neural basis of human error processing: reinforcement learning, dopamine, and the error-related negativity. *Psychol Rev*. 2002;109(4):679-709.

22. Miltner WHR, Braun CH, Coles MGH. Event-related brain potentials following incorrect feedback in a time-estimation task: evidence for a "generic" neural system for error detection. *J Cogn Neurosci*. 1997;9(6):788-798.

23. Holroyd CB, Baker TE, Kerns KA, Müller U. Electrophysiological evidence of atypical motivation and reward processing in children with attention-deficit hyperactivity disorder. *Neuropsychologia*. 2008;46(8):2234-2242.

24. van Meel CS, Heslenfeld DJ, Oosterlaan J, Luman M, Sergeant JA. ERPs associated with monitoring and evaluation of monetary reward and punishment in children with ADHD. *J Child Psychol Psychiatry*. 2011;52(9):942-953.

25. van Meel CS, Oosterlaan J, Heslenfeld DJ, Sergeant JA. Telling good from bad news: ADHD differentially affects processing of positive and negative feedback during guessing. *Neuropsychologia*. 2005;43(13):1946-1954.

26. Shiels K, Hawk LW Jr. Self-regulation in ADHD: the role of error processing. *Clin Psychol Rev*. 2010;30(8):951-961.

27. Williams J, Dayan P. Dopamine, learning, and impulsivity: a biological account of attention-deficit/hyperactivity disorder. *J Child Adolesc Psychopharmacol*. 2005;15(2):160-179; discussion, 157-159.

28. Montague PR, Dolan RJ, Friston KJ, Dayan P. Computational psychiatry. *Trends Cogn Sci*. 2012;16(1):72-80.

29. Meyer-Lindenberg A. From maps to mechanisms through neuroimaging of schizophrenia. *Nature*. 2010;468(7321):194-202.

30. Huster RJ, Debener S, Eichele T, Herrmann CS. Methods for simultaneous EEG-fMRI: an introductory review. *J Neurosci*. 2012;32(18):6053-6060.

31. Debener S, Ullsperger M, Siegel M, Engel AK. Single-trial EEG-fMRI reveals the dynamics of cognitive function. *Trends Cogn Sci*. 2006;10(12):558-563.

32. Rosa MJ, Daunizeau J, Friston KJ. EEG-fMRI integration: a critical review of biophysical modeling and data analysis approaches. *J Integr Neurosci*. 2010;9(4):453-476.

33. Oldfield RC. The assessment and analysis of handedness: the Edinburgh inventory. *Neuropsychologia*. 1971;9(1):97-113.

34. Petermann F, Petermann U. *HAWIK-IV: Hamburg-Wechsler–Intelligenztest für Kinder: IV.* 2nd ed. Bern, Switzerland: Hans Huber; 2008.

35. Waldmann H-C. Kurzformen des HAWIK-IV: Statistische Bewertung in verschiedenen Anwendungsszenarien. *Diagnostica*. 2008;54(4): 202-210.

36. Lidzba K, Christiansen H, Drechsler R. Conners Skalen zu Aufmerksamkeit und Verhalten–3: Deutschsprachige Adaptation der Conners; 3rd ed (Conners 3) von C. Keith Conners. Bern, Switzerland: Huber; 2013.

37. Kaufman J, Birmaher B, Brent D, et al. Schedule for Affective Disorders and Schizophrenia for School-Age Children–Present and Lifetime Version (K-SADS-PL): initial reliability and validity data. *J Am Acad Child Adolesc Psychiatry*. 1997;36(7):980-988.

38. Delmo C, Weiffenbach O, Stalder C, Poustka F. *Diagnostisches Interview Kiddie-Sads-Present and Lifetime Version (K-SADS-PL): 5: Auflage der deutschen Forschungsversion, erweitert um ICD-10-Diagnostik.* Frankfurt, Germany: Klinik für Psychiatrie und Psychotherapie des Kindes- und Jugendalters; 2001.

39. Rutter M, Bailey A, Lord C. *Social Communication Questionnaire (SCQ)*. Los Angeles, CA: Western Psychological Services; 2003.

40. Hauser TU, Iannaccone R, Stämpfli P, et al. The feedback-related negativity (FRN) revisited: new insights into the localization, meaning and network organization. *Neuroimage*. 2014;84:159-168.

41. Mathys C, Daunizeau J, Friston KJ, Stephan KE. A Bayesian foundation for individual learning under uncertainty. *Front Hum Neurosci*. 2011;5:39. doi:10 .3389/jnhum.2011.00039.

42. Vossel S, Mathys C, Daunizeau J, et al. Spatial attention, precision, and Bayesian inference: a study of saccadic response speed. *Cereb Cortex*. 2014;24(6):1436-1450.

43. Iglesias S, Mathys C, Brodersen KH, et al. Hierarchical prediction errors in midbrain and basal forebrain during sensory learning. *Neuron*. 2013;80 (2):519-530.

44. Stephan KE, Penny WD, Daunizeau J, Moran RJ, Friston KJ. Bayesian model selection for group studies. *Neuroimage*. 2009;46(4):1004-1017.

45. Delorme A, Makeig S. EEGLAB: an open source toolbox for analysis of single-trial EEG dynamics including independent component analysis. *J Neurosci Methods*. 2004;134(1):9-21.

46. Zottoli TM, Grose-Fifer J. The feedback-related negativity (FRN) in adolescents. *Psychophysiology*. 2012;49(3):413-420.

47. Cohen JD, Aston-Jones G. Cognitive neuroscience: decision amid uncertainty. *Nature*. 2005;436(7050):471-472.

48. Cohen JD, McClure SM, Yu AJ. Should I stay or should I go? how the human brain manages the trade-off between exploitation and exploration. *Philos Trans R Soc Lond B Biol Sci*. 2007;362(1481): 933-942.

49. Luman M, Van Meel CS, Oosterlaan J, Sergeant JA, Geurts HM. Does reward frequency or magnitude drive reinforcement-learning in attention-deficit/hyperactivity disorder? *Psychiatry Res*. 2009;168(3):222-229.

50. Kennerley SW, Behrens TEJ, Wallis JD. Double dissociation of value computations in orbitofrontal and anterior cingulate neurons. *Nat Neurosci*. 2011;14(12):1581-1589.

51. Matsumoto M, Matsumoto K, Abe H, Tanaka K. Medial prefrontal cell activity signaling prediction errors of action values. *Nat Neurosci*. 2007;10(5): 647-656.

52. Hare TA, Schultz W, Camerer CF, O'Doherty JP, Rangel A. Transformation of stimulus value signals into motor commands during simple choice. *Proc Natl Acad Sci U S A*. 2011;108(44):18120-18125.

53. Soon CS, He AH, Bode S, Haynes J-D. Predicting free choices for abstract intentions. *Proc Natl Acad Sci U S A*. 2013;110(15):6217-6222.

54. Williams ZM, Bush G, Rauch SL, Cosgrove GR, Eskandar EN. Human anterior cingulate neurons and the integration of monetary reward with motor responses. *Nat Neurosci*. 2004;7(12):1370-1375.

55. Finger EC, Marsh AA, Mitchell DG, et al. Abnormal ventromedial prefrontal cortex function in children with psychopathic traits during reversal learning. *Arch Gen Psychiatry*. 2008;65(5):586-594.

56. Chantiluke K, Barrett N, Giampietro V, et al. Inverse effect of fluoxetine on medial prefrontal cortex activation during reward reversal in ADHD and autism [published online January 22, 2014]. *Cereb Cortex*. doi:10.1093/cercor/bht365.

57. Liston C, Malter Cohen M, Teslovich T, Levenson D, Casey BJ. Atypical prefrontal connectivity in attention-deficit/hyperactivity disorder: pathway to disease or pathological end point? *Biol Psychiatry*. 2011;69(12):1168-1177.

58. Gläscher J, Daw N, Dayan P, O'Doherty JP. States versus rewards: dissociable neural prediction error signals underlying model-based and model-free reinforcement learning. *Neuron*. 2010; 66(4):585-595.

59. Rutledge RB, Dean M, Caplin A, Glimcher PW. Testing the reward prediction error hypothesis with an axiomatic model. *J Neurosci*. 2010;30(40): 13525-13536.

60. Pessiglione M, Seymour B, Flandin G, Dolan RJ, Frith CD. Dopamine-dependent prediction errors underpin reward-seeking behaviour in humans. *Nature*. 2006;442(7106):1042-1045.

61. Poil S-S, Bollmann S, Ghisleni C, et al. Age dependent electroencephalographic changes in attention-deficit/hyperactivity disorder (ADHD) [published online February 2, 2014]. *Clin Neurophysiol*. doi:10.1016/j.clinph.2013.12.118.

62. Doehnert M, Brandeis D, Imhof K, Drechsler R, Steinhausen H-C. Mapping attention-deficit/ hyperactivity disorder from childhood to adolescence—no neurophysiologic evidence for a developmental lag of attention but some for inhibition. *Biol Psychiatry*. 2010;67(7):608-616.

63. Liechti MD, Maurizio S, Heinrich H, et al. First clinical trial of tomographic neurofeedback in attention-deficit/hyperactivity disorder: evaluation of voluntary cortical control. *Clin Neurophysiol*. 2012;123(10):1989-2005.

64. Shaw P, Eckstrand K, Sharp W, et al. Attention-deficit/hyperactivity disorder is characterized by a delay in cortical maturation. *Proc Natl Acad Sci U S A*. 2007;104(49):19649-19654.

65. Rubia K. Neuro-anatomic evidence for the maturational delay hypothesis of ADHD. *Proc Natl Acad Sci U S A*. 2007;104(50):19663-19664.

66. Rubia K, Overmeyer S, Taylor E, et al. Functional frontalisation with age: mapping neurodevelopmental trajectories with fMRI. *Neurosci Biobehav Rev*. 2000;24(1):13-19.

67. Christakou A, Gershman SJ, Niv Y, Simmons A, Brammer M, Rubia K. Neural and psychological maturation of decision-making in adolescence and young adulthood. *J Cogn Neurosci*. 2013;25(11): 1807-1823.

68. Cohen JR, Asarnow RF, Sabb FW, et al. A unique adolescent response to reward prediction errors. *Nat Neurosci*. 2010;13(6):669-671.

Supplementary Online Content

!

Hauser TU, Iannaccone R, Ball J, et al. Role of the medial prefrontal cortex in impaired decision making in juvenile attention-deficit/hyperactivity disorder.
JAMA Psychiatry. Published online August 20, 2014.
doi**:**10.1001/jamapsychiatry.2014.1093.

This supplementary material has been provided by the authors to give readers additional information about their work.

eMethods. Supplementary Methods

Probabilistic reversal learning task
The task was similar to the task described in Hauser et al.(2014)[1]. On each trial, the subjects had to select the one of two stimuli. One of the two stimuli had a reward probability of 0.8 while the other stimulus had a reward probability of only 0.2. The subjects had to learn the reward probabilities on a trial-and-error basis. After six to 10 correct (minimally three consecutive correct responses) responses, the reward probabilities reversed, to which the subjects then had to adapt. The participants knew about the possibility of reversal, but they were not informed about any details of the reversals. Rewards were depicted by a framed 50 Swiss Centimes coin. As punishment, the participants lost 50 Swiss Centimes. The task consisted of two runs with 60 trials each. Participants were instructed to win as much money as possible. They knew that half of the money won was paid to them at the end of the study. On each trial, two objects were presented for 1500ms. One of the stimuli (the "correct" stimulus) had a reward probability of 0.8 and a punishment probability of 0.2. The other, "incorrect" stimulus had a punishment probability of 0.8 and a win probability of 0.2. Late answers (>1500ms) were punished with one Swiss Franc. This was done to prevent late answers and these trials did not enter the learning analysis. The average total trial duration was 9000ms. In each run, we additionally presented 20 null trials of 9000ms length.

Computational models
To infer behavior, we tested two learning models and two decision models. We performed model comparison using Bayesian random effects analysis[2]. The best performing model combination over all participants was used for group comparison and further analyses.
To ensure that participants did not respond randomly, performing at chance level, we additionally built a simple model without any free parameter which always resulted in a choice probability of 0.5 at every trial. This chance model was compared to the best performing of the other models. If the chance model performed equally well or better, we excluded this subject from analysis, given that no learning was detectable.

Learning models
We compared two different models which are explained in what follows. Note that, for clarity, we use δ for the RPE during outcome and choice value $V^{(t)}_{chosen}$ for RPE during cue presentation (because RPE$_{cue}$ is the difference between the expected value of the cue and not presenting a cue, which equals zero). For a more detailed explanation of this notational choice, see e.g., Niv et al. (2012)[3]. In the results and discussion sections, we use RPE$_{cue}$ for the expected value (V_{chosen}) and RPE$_{outcome}$ for δ.

Anticorrelated Rescorla-Wagner model
δ at each trial t was computed as the difference between the anticipated ($V^{(t)}_{chosen}$) and the received ($R^{(t)}$) outcome:

$$\delta^{(t)} = R^{(t)} - V^{(t)}_{chosen} \tag{1}$$

The values of both options were then updated using δ[4]:

$$V^{(t+1)}_{chosen} = V^{(t)}_{chosen} + \alpha\delta^{(t)} \tag{2}$$

$$V^{(t+1)}_{unchosen} = V^{(t)}_{unchosen} - \alpha\delta^{(t)}, \tag{3}$$

where α depicts the learning rate. The priors for the model fitting procedure were set to $V^{(0)} = .5$, $\alpha = .5(10)$ (mean(variance in logit space)).

Hierarchical Gaussian Filter model (HGF)
The HGF is a generic hierarchical, approximately Bayes-optimal learning model. The HGF fully complies with the assumptions of predictive coding and the Bayesian brain hypothesis, which states that the brain always learns in a Bayes-optimal fashion, given individually different priors[5,6]. The exact formulation, the model inversion and the complete update equations are described in Mathys et al. (2011)[7–9]. The HGF, as used here, consists of a hierarchy of 3 hidden states, where the states at levels 2 and 3 (x_2, x_3, resp.) evolve as Gaussian random walks over time (Figure 1B). x_1 ($\in \{0,1\}$) indicates the environmental state that defines which stimulus is being rewarded. It is governed by the state x_2 ($\in \{-\infty\infty\}$), which is transformed to the probability that x_1 by a logistic sigmoid transformation

$$p(x_1^{(t)} \mid x_2^{(t)}) = s(x_2^{(t)})^{x_1^{(t)}}(1 - s(x_2^{(t)}))^{1 - x_1^{(t)}} \tag{4}$$

with $s(x) := (1/(1 + e^{-x}))$. State x_2 evolves over time and is determined by a Gaussian random walk. The value of $x_2^{(t)}$ is normally distributed with mean $x_2^{(t-1)}$ and variance $e^{\kappa x_3^{(t)} + \omega}$

$$p(x_2^{(t)}) \sim N(x_2^{(t-1)}, e^{\kappa x_3^{(t)} + \omega}) \tag{5}$$

Since the variance of this random walk can be taken as a measure of the volatility of x_2, the log-volatility $\kappa x_3^{(t)} + \omega$ has two components, one phasic and the other tonic: x_3 is a state-dependent (phasic) log-volatility, while ω is a free parameter defining a subject-specific (tonic) log-volatility. κ was fixed to 1 as in Vossel et al. (2013)[8]. The state $x_3^{(t)}$ is normally distributed with mean $x_3^{(t-1)}$ and variance ϑ. ϑ is a free parameter and can be regarded as a subject-specific meta-volatility.

$$p(x_3^{(t)}) \sim N(x_3^{(t-1)}, \vartheta) \tag{6}$$

The variational inversion of the model yields subject-specific Gaussian belief trajectories about x_2 and x_3, represented by their means μ_2, μ_3 and variances (or, equivalently, precisions) σ_2, σ_3 (π_2, π_3). This inversion revealed that the trial-by-trial update equations highly resemble the update equations from Rescorla-Wagner models (cf. equation 1):

$$\delta_1^{(t)} = R^{(t)} - s(\hat{\mu}_2^{(t)}), \tag{7}$$

where $\hat{\mu}_2^{(t)} = \mu_2^{(t-1)}$ is the trial-by-trial mean of the Gaussian prior at the second level and $R^{(t)} := x_1^{(t)}$. $\hat{\mu}_2^{(t)}$ is updated by a precision-weighted RPE

$$\hat{\mu}_2^{(t+1)} = \mu_2^{(t)} = \hat{\mu}_2^{(t)} + \sigma_2^{(t)} \delta_1^{(t)}, \tag{8}$$

where $\sigma_2^{(t)}$ is the trial-by-trial variance at level 2. It can be expressed by a ratio of precision estimates $\hat{\pi}$

$$\sigma_2^{(t)} = \frac{\hat{\pi}_1^{(t)}}{\hat{\pi}_2^{(t)} \hat{\pi}_1^{(t)} + 1}, \tag{9}$$

$$\hat{\pi}_2^{(t)} := \frac{1}{\sigma_2^{(t-1)} + e^{\mu_3^{(t-1)} + \omega}}, \tag{10}$$

$$\hat{\pi}_1^{(t)} := \frac{1}{s(\mu_2^{(t-1)})(1 - s(\mu_2^{(t-1)}))} \tag{11}$$

For the update equations at level 3 and for the derivation of the equations, please refer to Mathys et al. (2011)[7]. Parameters were estimated in spaces where they were unbounded (e.g., the initial values σ_0 of the variances were estimated in logarithmic space, where their possible values are unbounded, while in native space there is a lower bound at zero). This enabled the use of Gaussian priors, which (in the appropriate spaces) were set to μ₀=[0,1](0,0), σ₀=[0,0](1,1), κ=1(0), ω=-2(10), ϑ=.03(1).

To sum up, the HGF has a similar update structure as the anticorrelated Rescorla-Wagner model (cf. equations 1 and 2 with 7 and 8). But instead of a fixed learning rate across the whole experiment (i.e., α), the learning rate is determined by an estimate of the variance of the belief (eq. 9). Therefore, the impact of the RPEs (δ₁) is modulated by the environmental volatility and the certainty of beliefs, resulting in a bigger impact of RPEs in more uncertain trials.

For a better understanding of this model in the context of RPE-theories, we define $\hat{\mu}_2^{(t)}$ of the chosen object as the choice value ($V_{chosen}^{(t)}$) and δ₁ as RPE. We decided not to investigate higher-order updates and beliefs because we had no specific hypotheses about these levels of the model.

Decision models

We combined each of the learning models with two of the most commonly used decision models. As first model, we chose a softmax function,

$$p(A) = \frac{1}{1 + e^{-\beta(V_A - V_B)}} \, ,$$

(12)

where $p(A)$ denotes the probability of choosing object A and β is a free parameter. As a second decision model, we implemented a unit square sigmoid transformation

$$p(A) = \frac{V_A^\xi}{V_A^\xi + V_B^\xi} \, ,$$

(13)

where ξ denotes the free parameter.

The main difference between these two models is how they translate beliefs into action probabilities. The softmax model is more flexible, especially in decisions with beliefs of high certainty, where the unit square model is (almost) deterministic. So far, the softmax model has mainly been used to model reversal learning tasks[1,4,10]. Nevertheless, with this comparison, we wanted to ensure that this decision model is also well suited for our data.

Model fitting procedure
All models were implemented and estimated using the HGF toolbox framework (v2.1; http://www.translationalneuromodeling.org/tapas/). We used the (negative) variational free-energy F to compare the model fits. F is a lower bound on the log-model-evidence, and the maximization of F therefore minimizes the Kullback-Leibler divergence between the exact and the approximate posterior distribution[11]. For optimization, we used the Broyden, Fletcher, Goldfarb and Shanno (BFGS) quasi-Newton optimization algorithm. We compared each combination of a learning model with a decision model using Bayesian model selection (BMS)[2]. Because the two groups could have had a different winning model, we ran BMS for all subjects together as well as for each group independently.

Data acquisition
We recorded fMRI in a 3 T Philips Achieva Scanner (Philips Medical Systems, Best, the Netherlands), which was equipped with a receive-only 32-element head coil array. We used an echo planar imaging (EPI) sequence which was optimized for maximal orbitofrontal signal sensitivity (TR: 1850ms, TE: 20ms, 15° tilted downwards of AC-PC, 40 slices, 2.5*2.5*2.5mm voxels, 0.7mm gap, FA: 85° FOV: 240*240*127mm). For normalization purposes we also acquired a T1-weighted structural image. For our simultaneous EEG acquisition, we used two MR-compatible 32-channel DC amplifiers (BrainProducts GmbH, Gilching, Germany). We recorded the data with a sampling rate of 5 kHz (recording reference: Fz, EEG recording filters: DC-250 Hz, ECG: DC-1000 Hz) from 63 scalp electrodes and 2 ECG channels. The 63 scalp electrodes covered the international 10-20-system[12] plus the following positions: FPz, AFz, AF2, FCz, CPz, POz, Oz, Iz, F5/6, FC1/2/3/4/5/6, FT7/8/9/10, C1/2/5/6, CP1/2/3/4/5/6, TP7/8/9/10, P5/6, PO1/2/9/10, OI1/2, left and right eye (laterally and below the eyes). For a more even coverage, O1'/2' and FP1'/2' were located 15% more laterally to Oz/FPz.

fMRI analysis
For fMRI preprocessing and analysis, we used SPM8 (http://www.fil.ion.ucl.ac.uk/spm/). The raw data were realigned, resliced, and coregistered to the T1 image. For normalization, the deformation fields were used, which were obtained using new segmentation. This procedure resulted in a new standard voxel size of 1.5*1.5*1.5mm. Subsequently, the data were spatially smoothed (6mm FWHM kernel).
For our fMRI analysis, we estimated the RPEs and choice values using the winning model across all participants. In the first-level GLM, we entered the model-derived RPEs (RPE$_{outcome}$, here δ_1) at feedback onset and choice values (RPE$_{cue}$, here $\hat{\mu}_2$) at cue presentation as parametric modulators. Additionally, we entered the following regressors of no interest to improve model validity. To control for movement-induced effects, we entered the realignment-derived movement parameters. Furthermore, we entered an additional regressor for each scan with a scan-to-scan motion > 1mm (determined using a custom adaptation of the artRepair-toolbox, http://cibsr.stanford.edu/tools/human-brain-project/artrepair-software.html). Because the heart rate is known to differ between ADHD and controls in reinforcement paradigms[13] and because pulsations induce micro-movements and therefore add noise to the data, we additionally regressed out pulsatile effects using an adaptation of RETROICOR (http://www.translationalneuromodeling.org/tapas/)[14,15]. Missing answers were also entered into a regressor-of-no-interest. For all task-related regressors, the spatial and temporal derivatives were enabled. Results of the random-

effects fMRI analyses are reported using a p<.05 voxel-height FWE threshold for task main effects, and p<.05 cluster-extent FWE correction (voxel-height threshold p<.001) for between group comparisons.

RPE main effects and group differences
To analyze the neural correlates of RPE processing during cue presentation and outcome (task main effects), we entered all subjects into one random effects analysis. To obtain the group differences, we compared both groups using independent t-tests (separately for RPE_{cue} and $RPE_{outcome}$).

Neural correlates of β
We evaluated where in the brain the decision steepness (model parameter β) is processed. To do so, we ran a covariate analysis during cue presentation with β as covariate in all subjects. To eliminate between-group effects, we added the group as an additional covariate-of-no-interest.

ROI-Analysis of sgACC/VS-cluster
ADHD – in particular with respect to decision making – has often been associated with activation differences in the ventral striatum[16]. We therefore decided to investigate the activity in this area, which is well known for processing RPEs[17–19]. In our RPE main effects analysis (RPE_{cue} and $RPE_{outcome}$ combined), we found a significant cluster containing the subgenual ACC and ventral striatum (sgACC/VS) to be activated by RPEs (cf. eFigure 2, 3E, eTable 3). We defined the ROI (8mm sphere) based on the peak voxel in the sgACC/VS cluster of our task main effects analysis (eFigure 2A, eTable 3). The effects of RPEs were computed using rfxplot[20]. We performed a split-half analysis of the RPE trials (hereafter: positive and negative RPEs) and used repeated measures ANOVAs and post hoc t-tests to compare the RPEs. The same analysis was also conducted based on a peak voxel from an independent group of healthy adults (n=25, 29.9y±7.4, 16m/9f) which played the same task. Their data were analyzed in the same way as described above. We also found a strongly significant main effects RPE activation in the sgACC/VS area (MNI: x=-5, y=17, z=-14; t(24)=6.53) and used this peak as the center of the ROI.

Functional connectivity analysis
To better understand how the impairments in the mPFC can be related to the sgACC/VS-impairment, we performed an exploratory connectivity analysis. We entered the SPM-derived first-level GLMs into the CONN-fMRI functional connectivity toolbox (v13p, http://www.nitrc.org/projects/conn/). Additionally, we entered the segmented structural images (gray matter, white matter, cerebro-spinal fluid) into the analysis for additional motion correction. The data were filtered using .008-.09Hz bandpass filter and we performed a ROI-to-ROI functional connectivity analysis (bivariate regression) using the mPFC clusters which were found to be impaired in the main RPE analysis. Additionally, the sgACC/VS-ROI was entered.

EEG preprocessing, analysis, and source localization
We used BrainVision Analyzer 2.0.2 (BrainProducts GmbH, Gilching, Germany) for EEG preprocessing. MR artifact correction was conducted using sliding average subtraction[21]. Cardioballistic artifacts were removed using the implemented CBC correction algorithms. The data was resampled (256 Hz) and filtered (.1 Hz-30 Hz, 50 Hz notch). Ocular and remaining cardioballistic artifacts were excluded using independent component analysis (ICA). The continuous data was re-referenced to average reference[22] and then exported for further analysis to Matlab using the eeglab-toolbox[23].
We used a peak-to-peak analysis to define the FRN. We segmented (-100-700ms relative to feedback onset) and baseline-corrected (-100-0ms) the continuous data in reward and punishment trials separately. Epochs with amplitudes greater than ±80μV were excluded from subsequent analyses (number of trials excluded: ADHD: 21±26, controls: 15±17, t(36)=.81, p=.426). We restricted our analysis to the electrodes Cz, FCz, and Fz, which are most often used in FRN analyses. For each subject, we determined the most negative peak between 200-425ms (punishment: ADHD: 316ms±43, controls: 323ms±46, t(36)=.43, p=.670; reward: ADHD 339ms±34, controls: 331ms±38, t(36)=-.71, p=.485) and the most positive preceding peak between 150-300ms (punishment: ADHD: 203ms±34, controls: 206ms±34, t(36)=.28, p=.780; reward: ADHD: 213ms±30, controls: 208ms±32, t(36)=-.55, p=.589), similar to the study by Zottoli and Grose-Fifer (2012)[24]. To determine the electrode with the maximal feedback-related response, we selected the electrode with the biggest difference between the two peaks. For both groups, electrode Fz elicited the biggest feedback-related response (Cz: $controls_{reward}$: -5.15μV±2.47, $controls_{punishment}$: -4.82μV±2.51, $ADHD_{reward}$: -5.63μV±3.23, $ADHD_{punishment}$: -5.15μV±2.65; FCz: $controls_{reward}$: -6.46μV±2.68, $controls_{punishment}$: -6.66μV±3.27, $ADHD_{reward}$: -7.53μV±3.67, $ADHD_{punishment}$: -6.54μV±3.60; Fz: $controls_{reward}$: -8.06μV±3.04, $controls_{punishment}$: -9.74μV±3.90, $ADHD_{reward}$: -8.81μV±4.08, $ADHD_{punishment}$: -

8.21μV±4.55, eFigure 2). We calculated the FRN by subtracting rewards from punishments and compared the FRN between the groups using independent t-tests.

To localize the FRN, we took the single-trial amplitudes and used them as a parametric modulator at the time of feedback in the first-level fMRI-GLM. We additionally entered all the regressors mentioned above (with exception of $RPE_{outcome}$) to improve model fit. We set the significance level to p<.001 cluster-extent FWE correction (voxel-height threshold p<.005) and localized the FRN in both groups independently.

eResults. Supplementary Results

Neural correlates of RPE processing: main effects

When analyzing the main effect of RPEs (cue and outcome combined), we found a network which showed increasing activation with increasing RPEs containing the ventromedial prefrontal cortex (vmPFC), posterior cingulate cortex (PCC), amygdala, lateral prefrontal cortex (latPFC), and a cluster containing the subgenual anterior cingulate cortex and the ventral striatum (sgACC/VS; eFigure 2A, eTable 3). A network containing the anterior insula, mPFC, latPFC, dorsolateral prefrontal cortex (dlPFC), inferior parietal lobe (IPL), precuneus, caudate, midbrain, and thalamus showed increasing activation with decreasing RPEs (eFigure 2B, eTable 3). For the RPE effects separated for cue and outcome, please refer to Figure 2.

Neural correlates of the decision steepness

Because we found differences in our model parameter β which indicates the steepness of the decision function (i.e. how exploratorily a subject behaves), we wanted to determine its neural correlates. Our covariate analysis revealed a network which contains mPFC, latPFC, dlPFC, STG and precentral area (eFigure 2C-D, eTable 3). These regions are well known regions of the decision making network: especially the mPFC has been associated with value comparison and response selection[25–27].

Analysis of sgACC/VS-ROI

The analysis of our sgACC/VS-ROI revealed a significant RPE (negative, positive) * time (cue, outcome) * group (ADHD, controls) interaction ($F(1,36)=6.16$, $p=.018$). Post hoc t-tests revealed that there was no difference for RPE_{cue} (negative RPE: $t(36)=.17$, $p=.865$; positive RPE $t(36)=-.15$, $p=.883$, eFigure 3A). For $RPE_{outcome}$, there was a significant difference for negative ($t(36)=-2.83$, $p=.007$, eFigure 3B) and positive RPEs ($t(36)=2.84$, $p=.007$). Also for the analysis which was based on an independent adult sample (s. above), we found a significant RPE (negative, positive) * time (cue, outcome) * group (ADHD, controls) interaction ($F(1,36)=5.17$, $p=.029$). Post hoc t-tests revealed that there was no difference for RPE_{cue} (negative RPE: $t(36)=.070$, $p=.945$; positive RPE $t(36)=-.065$, $p=.949$, eFigure 3C). For $RPE_{outcome}$, there was a significant difference for negative ($t(36)=-2.55$, $p=.015$, eFigure 3D) and positive RPEs ($t(36)=2.54$, $p=.015$). Thus, both groups showed similar RPE activation patterns during cue presentation, but controls show stronger RPE activation than subjects with ADHD in the sgACC/VS during outcome.

Functional connectivity analysis

To understand whether the differences between the mPFC were related to the sgACC/VS-cluster, we performed a ROI-to-ROI connectivity analysis. We found a significant connectivity in both groups between $mPFC_{outcome}$ and the sgACC/VS (controls: $.326±.147$, $t(19)=9.91$, $p<.001$; ADHD: $.192±.137$, $t(17)=5.95$, $p<.001$; eFigure 3E) and between the $mPFC_{outcome}$ and $mPFC_{cue}$ (controls: $.395±.399$, $t(19)=4.43$, $p<.001$; ADHD: $.311±.377$, $t(17)=3.50$, $p=.003$). No significant connectivity was found between $mPFC_{cue}$ and sgACC/VS (controls: $.134±.467$, $t(19)=1.28$, $p=.214$; ADHD: $.126±.357$, $t(17)=1.49$, $p=.154$). A comparison between the groups revealed a significantly reduced connectivity in ADHD between the $mPFC_{outcome}$ and the sgACC/VS ($t(36)=2.89$, $p=.006$), but not in the other two comparisons ($mPFC_{outcome}$-$mPFC_{cue}$: $t(36)=.67$, $p=.510$; $mPFC_{cue}$-sgACC/VS: $t(36)=.06$, $p=.950$).

References

1. Hauser TU, Iannaccone R, Stämpfli P, et al. The Feedback-Related Negativity (FRN) revisited: New insights into the localization, meaning and network organization. *NeuroImage*. 2014;84:159-168.

2. Stephan KE, Penny WD, Daunizeau J, Moran RJ, Friston KJ. Bayesian model selection for group studies. *NeuroImage*. 2009;46(4):1004-1017. doi:10.1016/j.neuroimage.2009.03.025.

3. Niv Y, Edlund JA, Dayan P, O'Doherty JP. Neural prediction errors reveal a risk-sensitive reinforcement-learning process in the human brain. *J Neurosci Off J Soc Neurosci*. 2012;32(2):551-562. doi:10.1523/JNEUROSCI.5498-10.2012.

4. Gläscher J, Hampton AN, O'Doherty JP. Determining a role for ventromedial prefrontal cortex in encoding action-based value signals during reward-related decision making. *Cereb Cortex*. 2009;19(2):483-495. doi:10.1093/cercor/bhn098.

5. Dayan P, Hinton GE, Neal RM, Zemel RS. The Helmholtz machine. *Neural Comput*. 1995;7(5):889-904.

6. Friston KJ. The free-energy principle: a unified brain theory? *Nat Rev Neurosci*. 2010;11(2):127-138. doi:10.1038/nrn2787.

7. Mathys C, Daunizeau J, Friston KJ, Stephan KE. A bayesian foundation for individual learning under uncertainty. *Front Hum Neurosci*. 2011;5:39. doi:10.3389/fnhum.2011.00039.

8.   Vossel S, Mathys C, Daunizeau J, et al. Spatial Attention, Precision, and Bayesian Inference: A Study of Saccadic Response Speed. *Cereb Cortex N Y N 1991*. 2013. doi:10.1093/cercor/bhs418.

9.   Joffily M, Coricelli G. Emotional Valence and the Free-Energy Principle. *PLoS Comput Biol*. 2013;9(6):e1003094. doi:10.1371/journal.pcbi.1003094.

10.   Hampton AN, Bossaerts P, O'Doherty JP. The role of the ventromedial prefrontal cortex in abstract state-based inference during decision making in humans. *J Neurosci*. 2006;26(32):8360-8367. doi:10.1523/JNEUROSCI.1010-06.2006.

11.   Friston KJ, Mattout J, Trujillo-Barreto N, Ashburner J, Penny W. Variational free energy and the Laplace approximation. *NeuroImage*. 2007;34(1):220-234. doi:10.1016/j.neuroimage.2006.08.035.

12.   Jasper HH. The ten-twenty electrode system of the international federation. *Electroencephalogr Clin Neurophysiol*. 1958;10:370-375.

13.   Luman M, Oosterlaan J, Hyde C, van Meel CS, Sergeant JA. Heart rate and reinforcement sensitivity in ADHD. *J Child Psychol Psychiatry*. 2007;48(9):890-898. doi:10.1111/j.1469-7610.2007.01769.x.

14.   Kasper L, Marti S, Vannesjö SJ, et al. Cardiac Artefact Correction for Human Brainstem fMRI at 7 Tesla. In: *Proc Org Hum Brain Mapp*.; 2009.

15.   Glover GH, Li T-Q, Ress D. Image-based method for retrospective correction of physiological motion effects in fMRI: RETROICOR. *Magn Reson Med*. 2000;44(1):162–167. doi:10.1002/1522-2594(200007)44:1<162::AID-MRM23>3.0.CO;2-E.

16.   Plichta MM, Scheres A. Ventral-striatal responsiveness during reward anticipation in ADHD and its relation to trait impulsivity in the healthy population: a meta-analytic review of the fMRI literature. *Neurosci Biobehav Rev*. 2014;38:125-134. doi:10.1016/j.neubiorev.2013.07.012.

17.   Gläscher J, Daw N, Dayan P, O'Doherty JP. States versus rewards: Dissociable neural prediction error signals underlying model-based and model-free reinforcement learning. *Neuron*. 2010;66(4):585-595. doi:10.1016/j.neuron.2010.04.016.

18.   Rutledge RB, Dean M, Caplin A, Glimcher PW. Testing the reward prediction error hypothesis with an axiomatic model. *J Neurosci Off J Soc Neurosci*. 2010;30(40):13525-13536. doi:10.1523/JNEUROSCI.1747-10.2010.

19.   Pessiglione M, Seymour B, Flandin G, Dolan RJ, Frith CD. Dopamine-dependent prediction errors underpin reward-seeking behaviour in humans. *Nature*. 2006;442(7106):1042-1045. doi:10.1038/nature05051.

20.   Gläscher J. Visualization of group inference data in functional neuroimaging. *Neuroinformatics*. 2009;7(1):73-82. doi:10.1007/s12021-008-9042-x.

21.   Allen PJ, Josephs O, Turner R. A method for removing imaging artifact from continuous EEG recorded during functional MRI. *NeuroImage*. 2000;12(2):230-9. doi:10.1006/nimg.2000.0599.

22.   Lehmann D, Skrandies W. Reference-free identification of components of checkerboard-evoked multichannel potential fields. *Electroencephalogr Clin Neurophysiol*. 1980;48(6):609-621.

23.   Delorme A, Makeig S. EEGLAB: an open source toolbox for analysis of single-trial EEG dynamics including independent component analysis. *J Neurosci Methods*. 2004;134(1):9-21. doi:10.1016/j.jneumeth.2003.10.009.

24.   Zottoli TM, Grose-Fifer J. The feedback-related negativity (FRN) in adolescents. *Psychophysiology*. 2012;49(3):413-420. doi:10.1111/j.1469-8986.2011.01312.x.

25.   Hare TA, Schultz W, Camerer CF, O'Doherty JP, Rangel A. Transformation of stimulus value signals into motor commands during simple choice. *Proc Natl Acad Sci U S A*. 2011;108(44):18120-18125. doi:10.1073/pnas.1109322108.

26.   Holroyd CB, Coles MGH. The neural basis of human error processing: reinforcement learning, dopamine, and the error-related negativity. *Psychol Rev*. 2002;109(4):679-709.

27.   Kennerley SW, Behrens TEJ, Wallis JD. Double dissociation of value computations in orbitofrontal and anterior cingulate neurons. *Nat Neurosci*. 2011;14(12):1581-1589. doi:10.1038/nn.2961.

eFigure 1. Analysis of the FRN.

The FRN was computed as the difference of the amplitude difference between N2 and P2 peak between punishments and rewards.
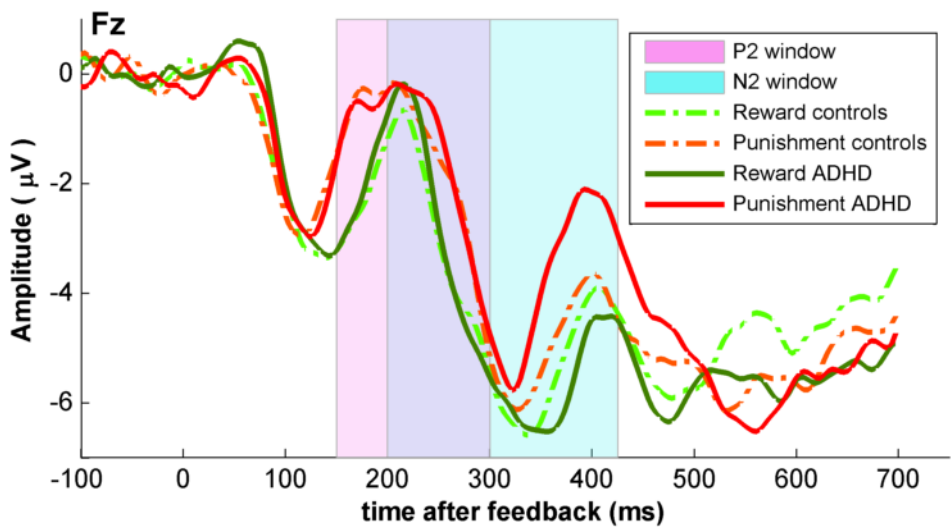
eFigure 2. Neural correlates of RPEs and decision function.

A, Increasing RPEs are associated with increased activation in a network containing the vmPFC and the sgACC/VS (p<.05 voxel-height FWE). B, Decreasing RPEs are associated with a network containing the anterior insula, mPFC and the dlPFC. The model parameter β, which indicates the steepness of the decision function, elicits a network containing the mPFC (C) and the latPFC (D) during the decision phase (p<.05 cluster-extent FWE).
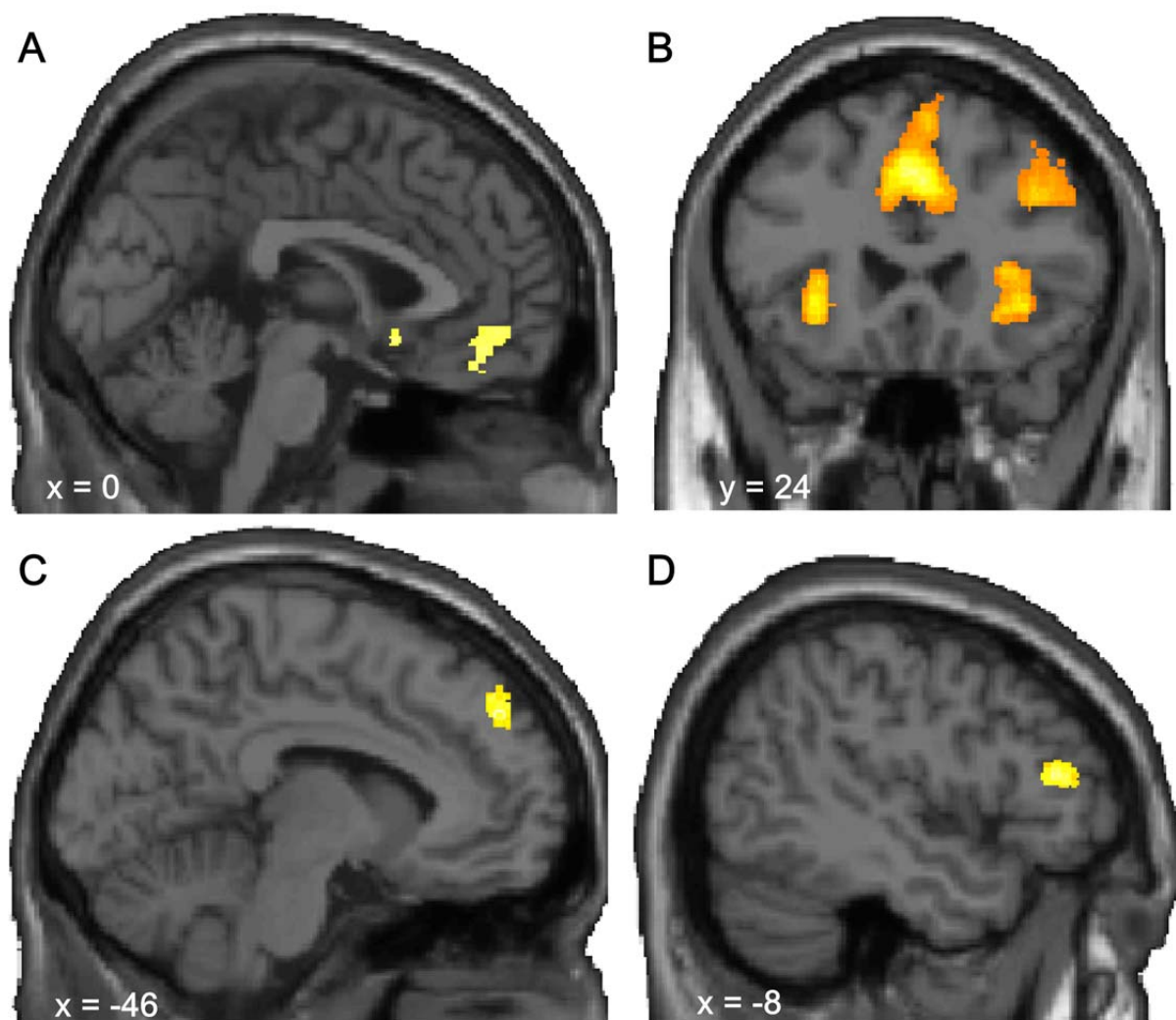
eFigure 3. Analysis of sgACC/VS-ROI and functional connectivity.

The analysis of a cluster in the subgenual ACC and ventral striatum (sgACC/VS) displayed no activation differences between the groups during cue-phase (A). However, during outcome phase (B), subjects with ADHD (red) showed no activation, while the healthy controls (black) showed normal modulation. The same held true when the ROI was based on the activation from an independent group of adults to analyze the RPE effects during cue (C) and outcome (D). (E) A functional connectivity analysis revealed a significant functional connectivity between the sgACC/VS-cluster and the mPFC (cluster derived from RPE$_{outcome}$ contrast between groups) in both groups. However, the functional connectivity was significantly decreased in ADHD compared to controls. * p < .05; ** p < .01; *** p < .001.
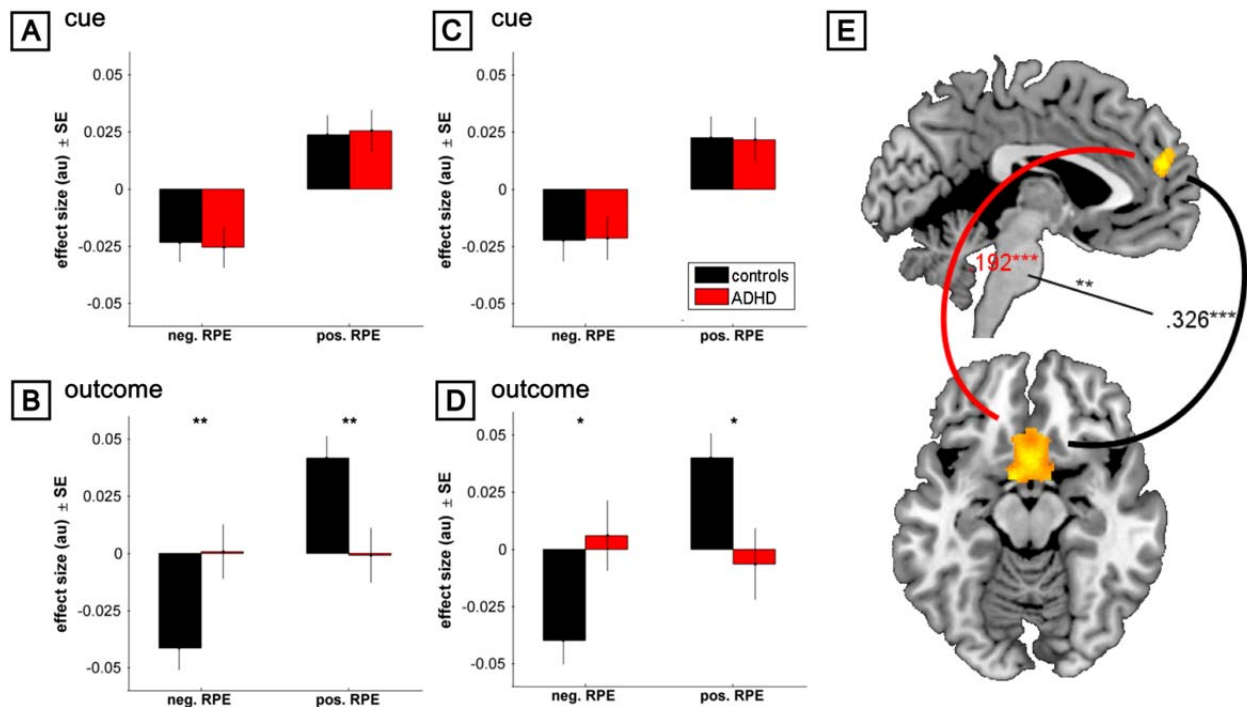
eTable 1. Behavioral differences between groups.

Analysis of reaction times and number of misses revealed no difference between the groups. This ensures that group differences found in modeling and earnings are not caused by reaction time differences between the groups (mean±std).

	controls	ADHD	
reaction time: mean	687ms±75	741ms±75	t(38)=1.43, p=.160
reaction time: standard deviation	178ms±37	197ms±44	t(38)=1.54, p=.132
misses	2.05±2.21	3.85±7.34	t(38)=1.05, p=.300

eTable 2. Results of the Bayesian model comparison.

The combination of the HGF learning model and the softmax decision model outperformed the other models for the whole group and for the healthy controls. For the ADHD patients, the anticorrelated Rescorla-Wagner model performed best. Please note that p_p and p_x sum up to 1 over the model space. Bold indicates the winning model. p_p: expected posterior probability; p_x: exceedance probability; RW: Rescorla-Wagner, sm: softmax decision model, usq: unit square decision model.

models	all subjects		ADHD		controls	
	p_p	p_x	p_p	p_x	p_p	p_x
anticorrelated RW - sm	.44	.30	.59	**.92**	.26	.02
anticorrelated RW - usq	.03	.00	.05	.00	.04	.00
HGF - sm	.51	**.70**	.32	.08	.66	**.98**
HGF - usq	.03	.00	.05	.00	.05	.00

eTable 3. Results of additional fMRI analyses: main task effect of RPE (cue + outcome) and decision steepness (model parameter β).

The RPEs elicit the typical activation found for RPE processing (regions reported at p < .05 voxel-height FWE, k > 10). Subjects with higher β show increased activations in these areas (regions reported at p < .05 cluster-extent FWE). Cluster size is given in number of voxels. Coordinates are reported in MNI space.

Contrast	Region	Hemisphere	Cluster size	x	y	z	z Score
RPE$_{cue+outcome}$	vmPFC	bilateral	435	-8	44	-12	6.38
	PCC	bilateral	373	-5	-55	19	6.37
	hippocampus/amygdala	right	21	15	-6	-20	5.85
			19	26	-16	-17	5.58
		left	18	-29	-19	-17	5.70
			12	-30	-34	-18	5.65
			12	-24	-24	-20	5.52
	latPFC	left	15	-51	32	7	5.74
	sgACC/VS	bilateral	20	0	14	-9	5.67
-RPE$_{cue+outcome}$	anterior insula	left	1035	-32	21	-8	>8
		right	1624	39	17	-6	>8
	mPFC	bilateral	3993	-6	27	39	>8
	latPFC	right	3451	26	53	-2	7.53
		left	773	-32	51	16	6.65
	IPL	right	1335	48	-45	40	7.14
			227	-39	-45	37	6.51
	precuneus	bilateral	420	8	-64	49	6.76
	caudate	left	118	-11	9	1	6.36
		right	238	15	18	1	6.33
	midbrain		202	-3	-24	-5	6.35
	thalamus	left	16	-11	-15	12	6.02
	dlPFC	left	39	-44	30	37	5.72
β	latPFC	right	197	63	15	9	4.75
		left	251	-48	35	12	4.44
	mPFC	bilateral	301	-8	48	37	4.56
	precentral	right	153	11	-25	73	4.48

		177	39	-15	33	4.13
STG	right	125	59	-24	7	4.32
dlPFC	left	92	-23	23	49	3.68